JPMTR-2412
DOI 10.14622/JPMTR-2412
UDC 667.2:535.6:676.2+678.7+66.095

Review paper | 194
Received: 2024-10-10
Accepted: 2024-12-27

# Natural plant dye inks set new challenges: analysing the interaction of anthocyanin-rich dye with modern calcium carbonate containing substrates

*Katarina Dimić-Mišić* [1,2], *Monireh Imani* [1,3] *and Patrick A.C. Gane* [1,4]

[1]School of Chemical Enhgineering,
Department of Bioproducts and Biosystems,
Aalto University, 00076 Aalto, Finland
[2]Institute of General and Physical Chemistry,
Studentski trg 12/V, 11158 Belgrade, Serbia
[3]Mirka Ltd., Pensalavägen 210, 66850 Jeppo, Finland
[4]Faculty of Technology and Metallurgy,
University of Belgrade, Karnegijeva 4, 11200 Belgrade, Serbia

katarina.dimic-misic@aalto.fi
monireh.imani@mirka.com
patrick.gane@aalto.fi

## Abstract

Plant dyes are increasingly finding applications across a broad spectrum of print technologies, leading to replacement of conventional synthetic dyes and pigmented inks for a range of print media. Despite technical advances, industrial application faces some fundamental challenges of achieving the necessary critical print properties demanded when using such dyes. These include maintaining runnability, colour definition and fastness while retaining functional stability, the latter being particularly challenging since many prints are based on digital patterning adopting inkjet or flexographic methods. This study explores the fundamental interactions between an example pure dye ink, derived from Aronia melanocarpa, a member of the family Rosaceae commonly known as chokeberry, and specific substrate filler and coating components. Key interactive factors include ink formulation, the nature of dye chemistry in relation to substrate structure, its optical properties and constituent components. The acidity of the juice-based ink is mainly dependent on the amount of anthocyanin (ANC), a water-soluble phytochemical plant protective flavonoid, occurring together with other phenolic compounds. Novel experiments are reported in which interactive substrate components are isolated and studied directly in contact with the naturally acidic anthocyanin-rich ink. Coloration of the dye is confirmed to be pH-dependent, and, as a result, major challenges arise when acidic ink contacts alkaline substrate, which covers the majority of paper, board and cellulose-based packaging materials today, due to the dominance of calcium carbonate as the filler and coating pigment of choice. In parallel, dye imbibed into substrate pores surrounded by materials of contrasting refractive index lead to effective colour gamut changes as the ratio of transmitted light through dye and scattered light from surrounding materials changes. This effect is exemplified comparing high refractive index titanium dioxide ($TiO_2$) versus lower refractive index calcium carbonate ($CaCO_3$). Finally, a strategy is proposed aimed at controlling the interaction and enhancing the overall printing performance.

**Keywords:** Aronia melanocarpa, ANCs, inkjet printing, solar cells, rheology of printing inks, edible printing.

## 1. Introduction

Printing of biobased inks, derived from fruits and vegetables, have been attractive for numerous applications, including in food production, for smart packaging on flexible paper and board substrates and for highly functional photocatalytic devices (Hakim,, et al., 2024; Tahir and Saad, 2021). Employing the sensitivity of natural dyes to their environment has been the driver in the case development of smart packaging for food, providing the potential of indicating shelf-life of perishable goods, as summarised in the review by Singh, Gaikwad and Lee (2018), covering the study of anthocyanin (ANC) dye. Photoselectivity of natural dyes features in their

role in organic solar cell production. This latter example is currently of major importance, since the growth of modern industry is highly dependent on establishing the use of renewable raw material and energy sources. Existing natural resources for fuel continue to diminish, and the building of a renewable energy based sustainable economy is vital to fulfil the production, transportation, and industrial trade needs of a growing global population (Perišić,, et al., 2022). Solar energy is clearly among the fastest growing proposed methods of capturing renewable energy. The typical lifespan of modern solar panels is 20–30 years. However, as solar deployments increase, a significant wave of decommissioned panels is expected in the coming decades, creating a potential waste management challenge (Huang, et al., 2022). The industry continues to focus on recycling concepts and repurposing of materials from decommissioned panels in an an effort to create circular economy. One contribution to sustainability is the adoption of biobased inks and substrates (Wathon, et al., 2019).

Adhesion in the case of dye inks is additionally related to adsorption onto surfaces, and the capture of dye in this way is very important in defining the position of the dye on and in the substrate and as a separating function for dye from solvent. The required adhesion of inks to paper can be affected by ink formulation, i.e. colorants, solvents, and diluent or carrier vehicle, and its interaction with the substrate pore structure (Ridgway and Gane, 2005). The influence on ink colorant distribution and adhesion mostly depends upon the compatibility between the dye and the carrier vehicle system, concentration and degree of dispersion in the final ink (Jurič, et al., 2013) and in parallel, the adsorption properties onto the substrate material surfaces, and, in the case of porous substrates, including pore wall adsorption (Ridgway and Gane, 2005). Distribution on non-absorbent substrates is controlled by the wetting behaviour of the ink vehicle solvent and finally the film-forming ability of the ink binder resin and its molecular affinity for the substrate, whilst distribution on and within a porous substrate is influenced additionally by the degree of vehicle penetration, transporting colorant into the pore structure – all major features particularly important for sustainable functional printing (Arya, et al., 2024). Solvents can, therefore, affect the distribution of printing ink in two different ways, demanding designed control of both wettability and penetration. Optimal control of ink penetration into the substrate surface without complete loss into the bulk can assist physical and chemical bonding and generate maximum coloration efficiency (Gane and Koivunen, 2010; Koivunen and Gane, 2010). The pore space and chemical properties of particulate grain surfaces are, therefore, important properties of a porous print substrate. Printing technology also places different demands on the interaction of liquid ink and a substrate. One of the most challenging is that of inkjet, a technology that has many advantages when considering functional print applications, due to its flexibility in handling readily modified ink formulations, particularly dye-based inks, and in small quantities for specialisation (Gane, et al., 2021; Dimić-Mišić, et al., 2015). Droplets of ink on arrival at the surface of the substrate are subject to wetting and capillary forces resulting in the solvent vehicle part of the ink together with the ink dye becoming absorbed into the fine pore structure, and thus separated from pigments, or pigment aggregates, and solid phase binders larger the pores (Gane, et al., 2021).

In the field of health foods and nutraceuticals, phenolic acid and polyphenols in general are well known for their anti-oxidant properties (Ebrahimi and Lante, 2021). Many nutraceutical products use printing techniques, including 3D printing, to incorporate active agents. This is common when formulating tablets with alkali calcium carbonate as an excipient. In these cases, the pH sensitivity of dye molecules is also crucial (Cotabarren, Cruces and Palla, 2019). In this field, traditional remedies for hypertension based on these compounds have been gaining recent attention. Surprisingly, the finding that polyphenols lower blood pressure, although seeming to be quite recent, and certainly long after the ailment was defined via blood pressure measurement (1856), ancient peoples native to the Americas (Abnakians and Potawatomians) (Rousseau, 1945; Rousseau, 1947; Smith, 1933) were using it medicinally for the treatment of cold, but probably did not know the link to the cause of whatever symptoms they were displaying (Hellström, et al., 2010). Similarly, in Russia and Lithuania chokeberry fruits have been used as antisclerotic agents as well as a complementary remedy against high blood pressure (Henneberg and Stasrznewicz, 1993; Sokolov, 2000).

In light of the traditional uses of chokeberry, it has been recently confirmed that it is one of the most prolific sources among plant berries, from which typically ~ 100 mg can be recoverable from 100 g of the plant's berry fruit (Tolić, et al., 2015). The rich content in natural compounds like polyphenols, flavonoids, and antioxidants not only enhance the overall health of the plant but also fortify it, with the leaves and stems being of a robust and tough texture, diminishing their appeal to many pests (Sant'Anna, et al., 2013; Zdunić, et al., 2020; Živković, et al., 2020; Zhang, et al., 2023). Unlike softer plants that insects find easier to penetrate and feed on, the resilience of its foliage acts as a formidable physical barrier. We also study two examples of the dye from different geographical regions, and so the geographical distribution differences are partly explained from the history of the plants involved. The berry originally proliferated in the eastern parts of North America, concentrated in Eastern Canada, and arrived in Europe as late as around 1900, passing through Germany to the then

Soviet Union (Russia) around 1946, during which time the plant was established as a cultivar. Aronia plants display ready adaptability to diverse soil conditions and climates, a trait closely tied to their resilience against pests. This adaptability enables them to flourish in different environments, withstanding potential stressors that might compromise the health of other plants. More recently it is being cultivated also in East European and Scandinavian countries, with the genus name Aronia being used instead of the original colloquial name, chokeberry. Aronia is a member of the Rosaceae family, and the cultivars used for fruit production are from the species Aronia melanocarpa, Elliot (black chokeberry, Aronia noir) and Aronia arbutifolia, originally from North America now cultured in the Baltic countries (Mossberg, et al., 2005; McKay, 2001).

Aronia shrubs, capable of reaching heights between 2 to 3 m, produce umbels comprising approximately 30 small white flowers from May to June. These flowers eventually give rise to two types of berries: bright red berries (red chokeberry) or purple-black berries (black chokeberry) that have diameter typically 6 to 13 mm and a weight ranging from 0.5 to 2 g. Harvesting, which is typically mechanised, is between August and September (Živković, et al., 2020).

The main compounds in Aronia berry juice are benzaldehyde cyanohydrin, hydrocyanic acid, and benzaldehyde. Among the benzene derivatives mostly present are to be found benzylalcohol, 2-phenylethanol, phenylacetaldehyde, salicylaldehyde, acetophenone, 2′-hydroxyacetophenone, 4′-methoxyacetophenone, phenol, 2-methoxyphenol and methyl benzoate. ANCs, also present as a group of plant molecules, are the components responsible for the colour of various fruits and flowers, protecting the plants from damage due to UV radiation (Huang and Xu, 2023). Chemical aspects of ANC are defining the colour of juice and colour durability, and these aspects largely define utilisation of Aronia in food applications. The typically purple-black fruit is an abundant source of dye colorant, and so is of major interest in the forming of dye-based printing ink.

A current challenge when using plant-based dyes is to maintain their colour properties, which degrade as a function of enzymatic breakdown. The resulting observed browning of fruit products is naturally detrimental to the appearance since it results in an undesirable colour change. However, colorants rich in phenols when combined with high levels of co-pigment/pigment ratio show a remarkable colour stability. In this context, it was found that chlorogenic acid, at concentrations greater than that of the natural ANCs present, enhanced the colour intensity of Aronia juices, suggesting the participation of natural pigments present in fruits in maintaining a co-pigmentation process (Dangles, Saito and Brouillard, 1993). By contrast, catechins appear to have a negative effect on red colorants, quickly turning yellowish when the pH is increased, whilst the presence of sugars is not influencing the colour. At a given pH, colour stability mainly depends on the structures of ANCs and of colourless phenolic compounds. Colorants rich in acylated ANCs (purple carrot, red radish, and red cabbage) display great stability due to intramolecular co-pigmentation. In aqueous solutions, aglycones of ANCs, organic compounds, such as a phenol or alcohol, combined with the sugar portion of a glycoside which exist as five molecular components, are held in chemical equilibrium. The colour gamut can range from red flavylium cation, through colourless carbinol pseudo base, to purple quinoidal base, blue quinoidal anion, and yellowish chalcone (Dangles, et al., 1993). Anthocyanins derived from the respective aglycones (anthocyanidins), and the general structure (flavylium cation), are shown in Figure 1 a) and c) (Mary, et al., 2020). At acidic pH (pH 2.0), flavylium cation is the dominant form and has a strong absorption at 520 nm, displaying a red colour. Changes can occur as pH rises with the flavylium cation losing proton and

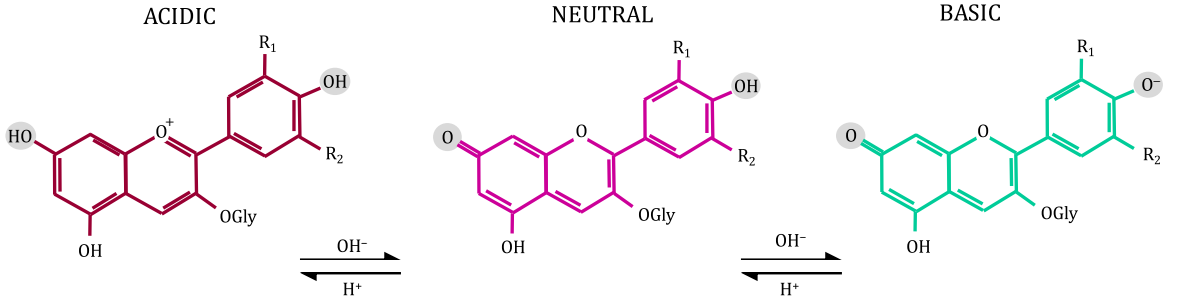


*Figure 1: Effects of pH of anthocyanin colour ranges and shift from red to blue at increasing pH; red colour that turns into purple at pH 1–5 (a), purple colour that turns into brown at neutral pH 6–9 (b), and green colour that turns to yellow at basic pH of 10–13 (c) [Figure taken and modified from (Mary, et al., 2020): [14] Open Access Article licensed under a Creative Commons Attribution-Non Commercial 3.0 Unported Licence – one change made applying equivalent chemistry replacing – $H^+$ with $OH^-$ to indicate the same addition of base.]*

gradually converting to quinoidal bases. The visible light spectral absorption becomes much weaker and shifts to 540–560 nm, yielding a red (pH 4.0) or a purple (pH 6.0) colour. At neutral pH, the blue quinoidal anion forms by losing another proton, and as a result reveals a stronger, red-shifted absorption reaching ~600 nm maximum. Ultimately, under basic conditions (pH > 8.0), i.e., passing through pH values typical of alkaline natural calcium carbonate, the flavylium cation will dehydrate to form colourless carbinol pseudo base and then chalcone. The chalcone form is yellow in colour, related to its absorption in the UV and violet-blue regions. The green colour of the anthocyanin solution at even higher pH 10.0 is derived from a resulting mixture of blue quinoidal anion and yellow chalcone (Mary, et al., 2020).

Upon digestion by endogenous enzymes in the human gastrointestinal tract, ANCs are released from the berry structure (Fu, et al., 2023). Anthocyanin in solution is changing both in respect to food health properties and in coloration as pH rises. During the progressive neutralisation of phenolic acids, a salt is formed. Under strongly alkaline conditions organic acids in general attach to sugar moieties and saponification occurs, which, in the case of the dyes considered here, results in acylation of the ANCs – typical of aliphatic acid acetylation.

Given the previously mentioned significant development in printing of edible vegetable dye inks on packaging paper and food substrates (Khan, et al., 2015; Fan, et al., 2019), clearly the preservation of coloration against pH degradation is already a topic of research. Similarly, as discussed here in this work, during drop-on-demand (DOD) inkjet printing on alkaline substrates partial ACN saponification may occur even if the eluted solution is immediately acidified (Dimić-Mišić, et al., 2015). In parallel, the use of natural dyes as photosensitisers is based on their large spectral absorption coefficients resulting in high light-harvesting efficiency, particularly in combination with $TiO_2$. Their natural renewable abundance, low cost and ease of preparation, whilst leaving no harm to the environment, means that their development in organic photoelectric devices is actively pursued, effectively eliminating concern of resource limitations.

In most of the cases introduced above, natural dyes' photoactivity is reliant on the presence of the ANC chemical family (Fan, et al., 2019; Mahmood, et al., 2018; Vandeput, 2021; Vatai, et al., 2008; Wathon, et al., 2019). However, when used as a dye in uncontrolled contact with a base there remains a major challenge, especially when faced by the ever-wider application of alkaline calcium carbonate. Natural dyes and calcium carbonate come into contact especially when the mineral is used as a filler in the food and paper industry, as well as in pharmaceuticals, mainly as functional excipient. This broad range of applications brings, newly, the concern in printing applications of anthocyanin-containing natural inks that they will exhibit discoloration. A strategy, therefore, is required to provide mitigation of this phenomenon, and to enhance the colour generation by application and substrate design. The work presented here illustrates the parameters at play during dye interaction with alkali substrate, so that such a strategy can be more reliably designed.

## 2. Material and methods

### 2.1 Aronia source, extract, and dye properties

Two different sources of Aronia fruit were used for investigating colour stability and printing. Aronia F (Northeast Finland) and Aronia L (Livonia – a historic region on the Eastern seaboard of the Baltic Sea in Latvia) with different compositions and colours (Figure 2). The extracts were obtained from clean fruits by crushing and dissolution using a pestle and mortar into a mixed solvent consisting of ethanol and water (1:1 in volume ratio). The samples were left at ambient temperature protected from exposure to direct sunlight to allow for adequate extraction of natural dyes in solution. It was found that consistent extract coloration was reached over a range of 3 to 5 days under these storage conditions. Solid residues were filtered out, and the clear solution was stored in a refrigerator at about +5 °C prior to printing (Velmurugan, et al., 2019).


*Figure 2: Image of two different types of Aronia melanocarpa berries extract, at pH 3.3*

### 2.2 Phenolic content measurement

Phenols, such as cyanidin-3-arabinoside, cyanidin-3-galactoside, (−)-epicatechin, chlorogenic and neochlorogenic acids, were analysed using high pressure liquid chromatography (HPLC). The stored methanolic extract from the Aronia was diluted by a factor of 100 with ACS (Attestation de Conformité Sanitaire: French attestation as potable) deionised water (supplied by Sigma-Aldrich, Merck Life Science OY, Keilaranta 6, 02150 Espoo, Finland) and filtered through a millipore

membrane filter (0.45 µm Nylon filter disk, Sigma-Aldrich). The HPLC apparatus (ESA Biosciences Inc., USA) consisted of a solvent delivery pump Model 582, guard cell Model 5010A (working electrode potential K1 = 600 mV, K2 = 650 mV), chromatographic column – Model Supelcosil LC8 (150.0 × 4.6 $mm^2$), 5 µm particle size and an electrochemical detector (Coulochem III). Chromatographic conditions were constant: 30 °C, mobile phase, being methanol and $H^2O$:$H^3PO^4$ = 99.5:0.5, (filtered through a filter Nylon, 0.2 µm, Sigma-Aldrich). The elution was isocratic, the flow rate of the mobile phase was 1.1 mL $min^{-1}$ following the procedures as reported by Miki, et al., (1995) and Hwang, Sakakibara and Miki (1981). The content of phenols was calculated as mg $kg^{-1}$ of fresh fruit mass.

### 2.3 Visualising the interaction with print substrate components

The interaction between the dye and substrate is primarily related to materials present in the substrate differing in pH from that of the acidic naturally occurring juice extract. Visualising the interaction is therefore undertaken using the individual component(s) responsible for the interaction both alone and in the composite structure of the substrate. Using this analytically designed approach allows us to deconvolute the material interactions from the multiple factors present in a ready-formed typical composite susbtrate.

#### 2.3.1 Mineral pigment tablet forming method and UV-visible spectrophotometric method

Model single component substrates, consisting purely of mineral pigments as found in high brightness paper and board, were formed as compacted fine particle tablets made from water suspensions of titanium dioxide ($TiO_2$), and calcium carbonate ($CaCO_3$), respectively, each at the mass fraction 0.5 of mineral solids content. The $TiO_2$ pigment suspension supplied as powder from Sigma-Aldrich was produced by mixing deionised water into the dry powder using a high speed Diaf mixer for 30 min (Pilvad Diaf AS, Præstemosevej 2, 4, 3480 Fredensborg, Denmark). $CaCO_3$ was supplied as a coarse wet ground (GCC) marble-based product, Hydrocarb 60 (the mass fraction 0.6 of particles < 2 µm), in aqueous dispersion by Omya AG, Switzerland. The tablets were constructed by wet filtration through a fine 0.025 µm filter membrane under pressure (20 bar) in a steel die, according to a method developed by Ridgway, Schoelkopf and Gane (2003). The tablets were then dried overnight at 60 °C. After drying, the tablets were ground to remove scratches/surface defects occurring on the edges and surfaces by a flat grinder. The tablets were stored under standard testing conditions at 23 °C, and relative humidity, RH, 50 % for 24 h prior to dye absorption studies using the dye extract as ink. The optical properties of Aronia ink drops applied to tablets made from $TiO_2$ and $CaCO_3$ were assessed spectroscopically. Light transmittance and absorbance measurements were made using a UV-visible spectrophotometer (Shimadzu Model 160-A, Kyoto, Japan) across the wavelength range of 300–800 nm. Notably, differences in spectral response among the two constituent inks could be observed, which were primarily attributed to variation of refractive index contrast between each ink and the surrounding mineral in the tablets.

#### 2.3.2 Change of pH effect arising from mineral pigment

Behaviour of Aronia dye as a function of mineral contact in combination with changing pH can be separated generally between low pH and mid-to-high pH conditions. At low pH, the potential for deprotonation of flavylium cations is suppressed, resulting in a lack of binding of ANC to flavylium cations, and possibly also preventing the binding of other dye components, due to charge repulsion. These changes can be induced by contact with mineral pigments (Asbury, et al., 2003). For example, when used in photosensitisers incorporating $TiO_2$ it was shown in solar cell application that lower observed short circuit photocurrent, $_{JSC}$, at basic pH may be explained by two different factors (Imanishi, et al., 2007). One of these is due to the decreasing driving force for electron injection caused by the upward shift of the conduction band edge of $TiO_2$ with increasing pH when used on printing paper and board, sometimes also containing some $TiO_2$, where the majority mineral is $CaCO_3$ alone (Asbury, et al., 2003; Imanishi, et al., 2007). This supports that contact with $CaCO_3$ mineral pigment results naturally in a rise of pH.

The natural pH was found to be 3.3 for Aronia F and 3.7 for Aronia L, similar to values reported by Skupien, Ochmian and Grajkowski (2008). Change in pH as a function of 0.1 M NaOH addition was monitored using a pH meter (SP-701, Suntex Instruments Co. Ltd., Kangning St., Xizhi Dist., New Taipei City, Taiwan). In addition to the impact of pH on dye properties, contact between acidic species and $CaCO_3$ results in the release of calcium ion, $Ca_2$+, which, in turn, can lead to coagulates forming with, and saponification of, the dyestuff. The effect of $Ca_2^+$ on ANC extract was studied by adding 3 M $CaCl_2$ to the samples of Aronia dye and measuring particle size development.

The coupled phenomena of pH change of Aronia inks, due to exposure to $Ca_2^+$ ions on contact with $CaCO_3$, and the resulting potential impact on coloration and colour fastness (stability of colour) are thus studied using the model substrates consisting of mineral pigment alone.

### 2.4 Inkjet printing process

In this study we used a lab scale DOD piezoelectric based inkjet printer, Fujifilm Dimatix material printer

DMP-2831 (Fujifilm Corp., Midtown, Akasaka, Minato, Tokyo, Japan) using the manufacturer's DMC-11610 ink cartridges with nominal 10 pL drop volume to realise a proof-of-concept study (Koivunen, Jutila and Gane, 2015; Dimić-Mišić, et al., 2015). Droplet jetting frequency of 1 kHz was applied to all the ink extracts and to evaluate uniformity and optical properties of printouts of the dye samples. Printing was performed at room temperature (23 °C).

### 2.5 Characterisation of printouts

Printing papers were provided by Stora Enso (Lumi - Press, 170 g/m$^2$ substance and 0.7 µm roughness). The information about uniformity and surface morphology of printed electrolyte patterns was determined with optical light microscope (Leica Microsystems).

### 2.6 Rheological Tests

Since inkjet printing, being one of the most likely technologies to be used, subjects ink to various flow conditions during pumping, ejecting, drop splitting and substrate surface flow it is important to evaluate its resistance to these applications of shear and strain, and of particular interest is the change of these properties over time in response to physical and chemical interactions.

Rotational instrumentation is commonly used to study the rheological response of liquids and colloidal suspensions to shear, depending on the rotation rate and gap between the elements defining the physical experimental boundaries. Parallel plate–plate confinement is one such typical liquid geometry, where, in this case, the sample was loaded onto the lower of the two parallel plates of a Physica MCR 301 rheometer, (Anton Paar, Graz, Austria), and the upper plate then lowered until the distance between the two plates was 0.5 mm. Temperature throughout the measurement was held at 23 °C, and an anti-evaporation cover was attached onto the rheometer upper plate to minimise measurement errors arising from the loss of solvent (water evaporation) during the experiment. The inks were initially subjected to a pre-shearing shear rate ($\dot{\gamma}$) of 50 s$^{-1}$ for 30 s, and left to rest stationary for 60 s. Shear rate ($\dot{\gamma}$) input values were ranged between 0.01 and 1 000 s$^{-1}$ to study the dynamic viscosity response ($\eta$) of the inks. Response of the dye solution to shear rate is critical during expulsion from the inkjet printer nozzle and in respect to flow on the substrate surface and absorption rate into pores, if present.

By applying controlled strain using electronic feedback, the derived internal stress in the sample can be determined (Duffy, et al., 2015). This method, without resorting to oscillation, is useful for retaining materials in suspension, where otherwise there might be sedimentation (Dimić-Mišić, et al., 2015; Mahmood, et al., 2018; Medina-Meza, et al., 2016). The stress response of the Aronia dye solutions is important both at the impulse time of pressure application to initiate droplet formation and upon impact with the substrate surface.

### 2.7 FTIR analysis

In the interests of understanding changes in chemical composition of the dyes as a function of pH, $Ca_2$+ exposure and physical shear samples were analysed using Fourier transform infra-red (FTIR) spectroscopy (Perkin Elmer, Revvity Finland OY, Mustionkatu 6, 20750 Turku, Finland) before and after shearing by forming dried ink films. The films were made by pouring a thin layer of suspension in a Petri dish and then drying at room temperature (23 °C), whilst protecting from direct light.

### 2.8 Particle size measurements

Size data were reported as particle diameter derived from time-averaged static light scattering as a function of scattering angle from a dilute dispersed suspension of particles using a Malvern Instruments Mastersizer (Malvern Pananalytic 3000 Ltd., Malvern WR14 1XZ, UK). The particle size distribution is represented by the volume of particles present having a size less than a given size, $d_{SV}$, e.g., the median volume based particle size is represented by the diameter of the particle for which the volume fraction 0.5 of particles are finer than d50 %.

## 3. Results and discussion

### 3.1 Phenolic content of Aronia extracts

The phenolic content, present in different amounts in the two geographically separate samples of Aronia melanocarpa, Aronia F (sourced from Finland) and Aronia L (sourced from Latvia), together with their chemical element analysis are presented in Table 1 and Table 2, respectively.

Both Aronia melanicarpa samples were rich in minerals, which relate to their well-known trace element nutraceutical properties and their antioxidant action (Kampuse, et al., 2009; Sarv, et al., 2021; Angelova, et al., 2017), with Aronia F ink having somewhat higher levels of Al, Na and K ions, Table 2.

### 3.2 Effect of pH and link to print application on modern $CaCO_3$ coated paper

As depicted in the Figure 3, the colour of the Aronia extract, as predicted, undergoes discernible changes with fluctuations in pH content. The observed variations highlight the pH-dependent nature of the extract, showcasing a dynamic interplay between pH levels

*Table 1: The most important constituents of Aronia melanocarpa extracts TPC = total phenolic content, TPAC = total phenolic acid content, TAC = total anthocyanin content is seen to differ in amount between Aronia F and Aronia L*

| Phenolic type and content in sample extract | Aronia F | Aronia L |
|---|---|---|
| TPC (mg GAL $L^{-3}$) | 12 857 ± 200 | 77 816 ± 106 |
| TPAC (mg GAL $L^{-3}$) | 919 ± 116 | 589 ± 96 |
| TAC (mg Gy-3 GalE $L^{-3}$) | 13 233 ± 167 | 8 312 ± 143 |

and the resultant coloration, as with increasing pH colour changes from purple to red then towards blue and greenish yellow. Figure 3a) illustrates the colour change as a function of pH controlled by addition of NaOH, as exemplified in the case of Aronia F ink extract.

By viewing the spreading of ~ 0.1 mL droplets of ink at each pre-adjusted pH level placed on calcium carbonate coated paper Figure 3b) reveals the formation of particulate material in the ink-on paper state starting at pH value 3.3 and extending to 8.7. However, less particulate matter is produced when the ink is applied at pH 10.4, and the consistency of dye coloration (yellow) is the purest of the series by being essentially free from particulates except for the image edges. The Marangoni effect, often referred to as the coffee stain effect, is clearly demonstrated here, whereby the progressively concentrating ink dye is transported, as a function of absorption into the porous coating and drying time, toward the droplet spread perimeter. This transport phenomenon also concentrates the coagulate particles formed in the presence of $Ca^{2+}$, being released from the $CaCO_3$ coating pigment. Additionally, colour dye component separation is clearly observable suggesting that a chromatographic process of adsorption to the $CaCO_3$ coating pigment particle surface may also be at play. Figure 3c) in turn demonstrates how the microscopic spread of printed inkjet dots eventually begins to lead to the desired full tone image on the paper surface.

### 3.3 Additional impact of exposure to $Ca^{2+}$

To illustrate the result arising from extended exposure of acidic Aronia dye inks to $CaCO_3$ typically found in modern papers as filler coating pigment, and suspected to have caused coagulation as seen previously in Figure 3, the ink extracts were mixed, respectively, with the $CaCO_3$ pigment suspension with the mass fraction 0.5 as was used as precursor to forming the mineral tablets (studied further in the section 3.6). The high brightness of the $CaCO_3$ suspension clearly dominates the colour of the mix, as shown in Figure 4 b) before and after Aronia L ink addition, but the ink nonetheless provided an observable tinge of col-

*Table 2: The chemical element analysis of elements present in the sample extracts of Aronia melanocarpa*

| Mineralic element | Ion content /mg $L^{-1}$ | |
|---|---|---|
| | Aronia F | Aronia L |
| Al | 121.1 | 95.7 |
| Fe | 23.9 | 22.9 |
| Mn | 13.6 | 25.1 |
| Mg | 954.4 | 963.3 |
| Ca | 1449.1 | 1729.7 |
| Na | 233.4 | 129.4 |
| K | 11 601.5 | 9306.3 |

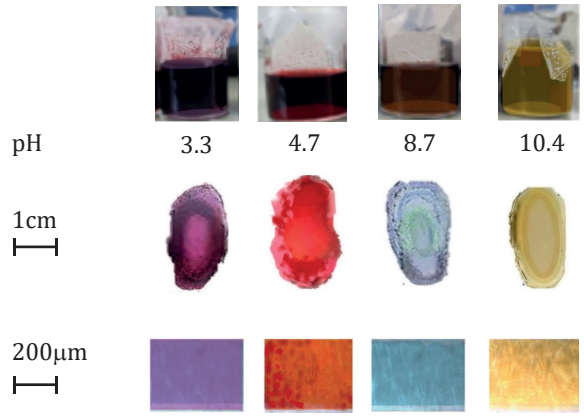


*Figure 3: Appearance of Aronia F ink at room temperature: a) change of pH in alcohol ink extracts causing change in colour, b) spreading of macroscopic ink droplets on contact with $CaCO_3$ coated paper substrate and c) optical micrographs of inkjet printed dots on paper showing their merging to form a solid full tone image by ink dot spreading*

oration to the eye. The mixed samples were placed for 24 h in refrigerated storage at 5 °C. Following this storage time, it was observed that a pink foam layer had formed in the neck of the glass storage vials. The foam product is illustrated in Figure 4 c), where the comparative colour is just discernible between the remaining bulk of the mixed suspension and the extracted foam-including layer. These effects reflect the combined impact of raised pH to that of naturally occurring $CaCO_3$ acting as buffer and the exposure to $Ca^{2+}$ resulting from the acid-base reaction. In addition, it was seen that the amount of foam, indicating acidic reactivity, was greater for the Aronia F versus Aronia L, which is in accordance with the higher acidic phenolic content in Aronia F.

To analyse further the chemical product arising from $Ca^{2+}$ reactivity alone the ink samples were treated by the addition of $CaCl_2$, and the difference in reactivity between the inks, related to $Ca^{2+}$ without excess base

present, was observed. In this case, contrary to when base is present, and in accordance with phenolic acid content, Table 1, ink in which ANC and phenols (TPC, TAC, TPAC) were less prevalent, and, hence, required less ionic exchange to coagulate, reacted faster and produced greater thickening with aging (Fan, et al., 2019; Khoo, et al., 2017; Vandeput, 2012). FTIR analysis revealed the suspected presence of additional species constituting calcium soap particles, Figure 4 a).

Formation of coagulates upon $CaCl_2$ addition was studied via monitoring the increase in particle size within the ink suspension. Figure 5 shows how the median particle size increases significantly when the ink was exposed to $Ca^{2+}$ ion, rising from a value ~ 60 µm to 68 µm and 72 µm, respectively, for Aronia F and Aronia L. Although this increase in median particle size might not in itself impact inkjet printing jettability, the real problem lies in the extension at the coarse end of the particle size distribution, where particles as large as 85–90 µm, which were not present in the original ink, not only appear, but have significant random occurrence, shown by the rise in the curve (insert in Figure 5) at this large particle size, particularly in the case of Aronia L. Of note also is the formation of a shoulder representing increased fine particles upon exposure to $Ca^{2+}$, seen as a shoulder to the left of the size distribution curves, Figure 5, for both inks. In the case of Aronia F the increase in fines ranges from around 38 to 53 µm, whereas that for Aronia L displays ultrafine particles generated over an even greater extended range from 25 to 50 µm. This suggests that the process includes not only a coagulating $Ca^{2+}$ bridging effect between acid groups of existing particles, leading to coarser particulates, but a seeding of fine insoluble salt particles arising from calcification of soluble acidic ink species.

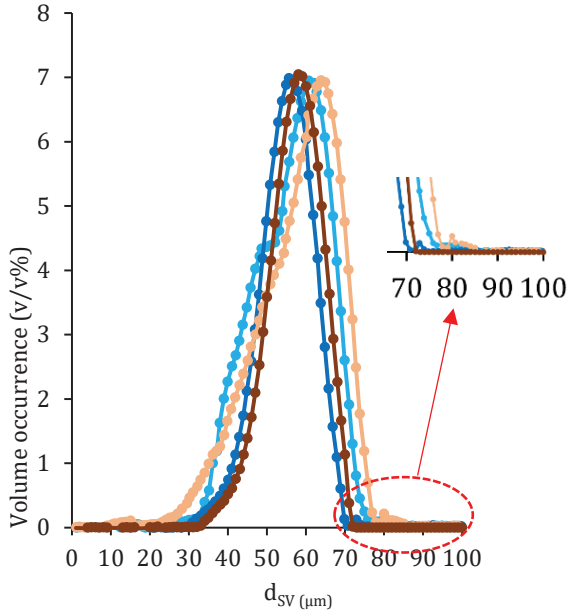


*Figure 5: Particle size distributions for the two Aronia inks F and L, comparing before and after the addition of $CaCl_2$, showing both formation of fine insoluble salt particles and the coagulation of existing particulate matter to form significantly larger particles*

### 3.4 Rheological effect of pH on ink stability

Controlling the viscoelastic behaviour of the inks is crucial for the jetting performance of the droplets in inkjet printing applications (Medina-Meza,, et al., 2016). Although in many inkjet printing studies only zero-shear rate viscosity of the inks has been presented for the initial jetting flow characteristics of the printing inks, based on the assumption of Newtonian behaviour, more measurement points need to be added into

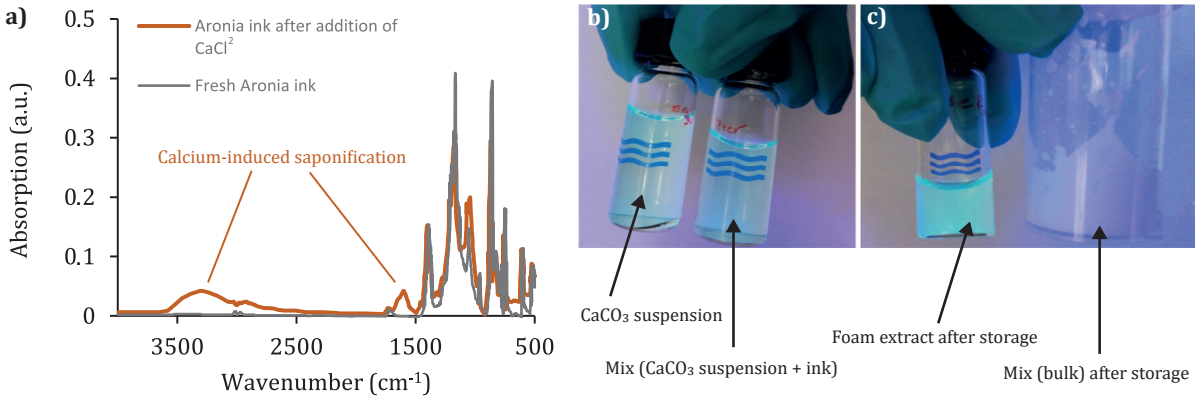


*Figure 4: a) FTIR spectra showing difference in molecular structure as a result of saponification and particle formation in Aronia ink extract upon addition of $CaCl_2$ before and after storage, b) mixing Aronia L ink with $CaCO_3$ suspension and c) separating the upper layer of foam from stored sample mix of $CaCO_3$ and Aronia F*

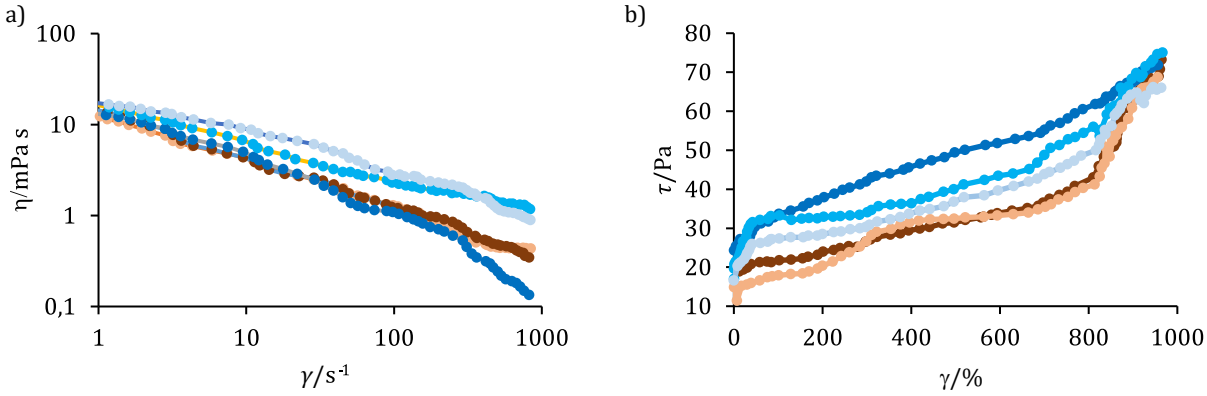


*Figure 6: Steady state response of Aronia inks, a) dynamic viscosity over the range of shear rate, and b) static stress response to strain*

the experiments in the case of non-Newtonian fluids (Dimić-Mišić, et al., 2015; Hashmi, et al., 2015). Dynamic viscosity measurements of the liquids indicated a shear thinning behaviour at low to medium shear rates, and thickening behaviour (dilatancy) at higher shear rates for those samples, suspected of containing concentrated particles in suspension (Dimić-Mišić, et al., 2015; Mahmood, et al., 2018). When considering inkjet nozzle function, dilatant behaviour is undesirable as it can result in clogging of nozzles, which directly disturbs printing performance (Mahmood, et al., 2018; Medina-Meza, Boioli and Barbosa-Cánovas, 2016). The greatest rheological stability was observed for inks at their natural pH, in acidic condition, with continuing shear thinning at the higher shear rates, Figure 6a). However, at the higher shear rates measured, the energy release is reflected in a strong growth of internal stress response to high levels of strain, Figure 6b). In contrast, inks adjusted to higher pH levels showed initial stress increase from the stationary state, but then did not dissipate excess energy at the highest strain levels, Figure 5b), displaying a monotonic stress behaviour upon increase in alkalinity.

Moreover, it is noteworthy to mention that the agglomeration phenomenon in the suspension would, once again, have practical implications, particularly in the context of formulation and manufacturing processes. The size and distribution of aggregates can affect the rheological properties, stability, and quality of the Aronia based products, such that inkjet printing would no longer be reliable in respect to jettability. Thus, considering pretreatment with $Ca^{2+}$ ion cannot be considered as viable for inkjet printing, and so was not analysed rheometrically in this study.

### 3.5 UV-Vis absorption spectra and optical effect on mineral coating pigment

The dye optical properties of the Aronia inks were evaluated using spectrophotometry across the ultraviolet (UV) and visible (Vis) light spectrum. Dyes deliver coloration by absorbing the complementary colours in the visible spectrum, thus transmitting light having the characteristic colour band of the dye only. Figure 7, a) and b), shows the optical absorbance and transmittance spectra, respectively, for the Aronia F and Aronia L inks across the wavelength range 300–800 nm.

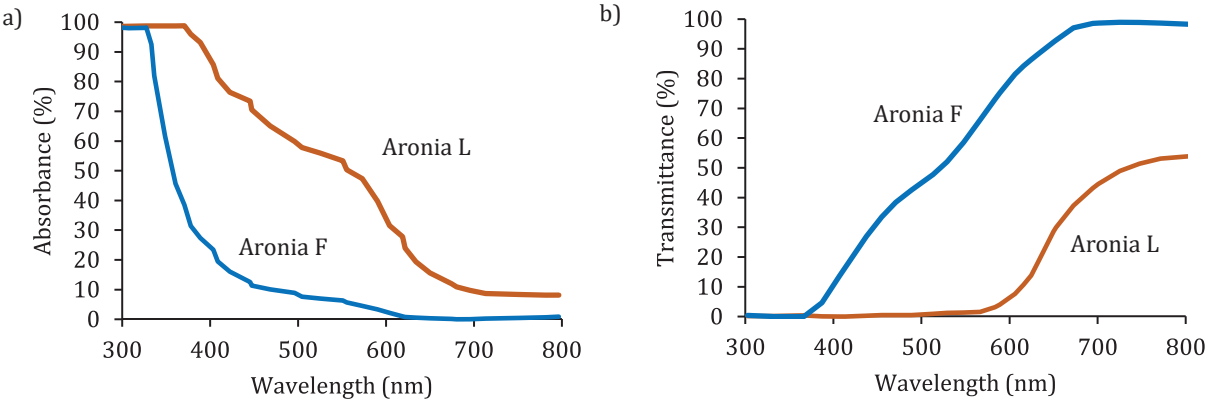


*Figure 7: Optical spectral properties of Aronia F and Aronia L dye extract inks, a) light absorbance, and b) light transmittance depending on the ratio of anthocyanin and total phenolic content of the inks Aronia F and Aronia L (Table 1)*

Comparing the light filtration properties of the dyes, the spectrometric absorbance and transmittance as a function of wavelength determine both the colour spectral response and the intensity or purity of the inherent dye coloration. Considering the spectra shown in Figure 7, a) and b), it is clearly possible to discern the distinct difference in breadth of the spectral response. The Aronia F dye contains more ANC and phenolic compounds (PC) in total, resulting in a more specifically active absorption at short wavelength compared with the broad spectrum absorbing Aronia L dye (Vandeput, 2021; Vatai, et al., 2008; Borowska, et al., 2020). These differences lead to the coloration print density reflectance properties of the combined system of dye on and penetrated within a porous substrate.

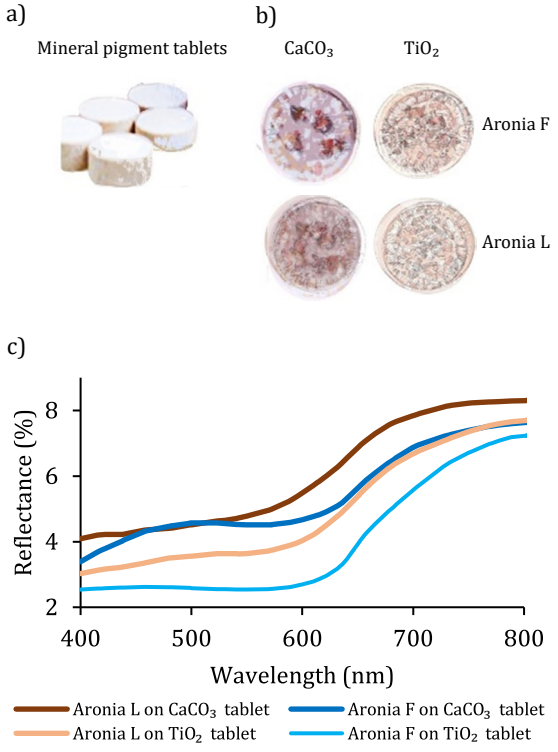


*Figure 8: a) Porous tablets formed from $CaCO_3$ and $TiO_2$ each at the mass fraction 0.5 of pigments in water suspension, b) images of ink droplets applied to the surface of $CaCO_3$ and $TiO_2$ based tablets (note the greater colour intensity for ink on $CaCO_3$ compared with $TiO_2$, c) diffuse spectral reflectance measured from the dye impregnated tablet area*

Drops of Aronia F and Aronia L inks were put onto the surface of the $CaCO_3$ and $TiO_2$ compression formed tablets (Figure 8a), respectively, and the ink in each case was clearly seen to be absorbed via capillary imbibition. Due to the necessarily higher porosity of the coarser particle size $CaCO_3$, volume penetration within the $CaCO_3$ tablet was more rapid. In both material cases, the colours of the tablets changed in response to the presence of the dye, with reactivity and change in pH being greater in the case of $CaCO_3$, as was expected (Figure 8b). Additionally, the points of applied ink on the $CaCO_3$ tablet appeared more intense on the $CaCO_3$ than on the $TiO_2$ tablet, even though ink penetration was faster for $CaCO_3$. This observation is important when considering the dye colour intensity desired for a given print, i.e. less ink is required when printed on the $CaCO_3$ to achieve the same print density. Upon comparison, the refractive index of $CaCO_3$ is typically ~1.51 whereas that of $TiO_2$ in the rutile form is almost double at 2.87, with a virtually complete light absorption at a wavelength of 632.8 nm having a transmission coefficient of 0.

The observed print density phenomena, relating to the coating material and structure, for a dye ink print predominantly centre on a combination of porous matrix light scattering, related to optimal pore size and pore occurrence at that size, versus surface light scattering and absorption as a function of high material refractive index. Thus, high light scattering from optimally sized pores (~ 0.2 µm for visible light) containing dye held within a matrix of bright low light absorbing $CaCO_3$ particles results in a greater amount of dye-filtered light returning to an external observer than the case where highly light absorbing $TiO_2$ masks the internal volume of the coating layer preventing light from entering the interparticle pores deeper in the porous matrix. Furthermore, the intense light back-scattered from the $TiO_2$ surface particle layer reduces the colour contrast even further due to high white light content returning to the external observer. This balance of contrasting light scattering properties of the porous substrate, combined with accessible dye performing light spectral filtration determines the coloration and intensity as measured by the spectrometer operating in diffuse reflection mode, Figure 8c). Interpreting the reflectance to define coloration intensity requires the observer to note the sharpness of specificity change in diffuse reflectance across the wavelength spectrum studied. A pure intense coloration is seen when the reflectance is low across much of the spectral range but rises sharply over one or more narrower spectral band(s), typical of the dye colour itself. Thus, studying the reflectance curve of Aronia F applied onto the $CaCO_3$ tablet in comparison to the others, reveals distinct specificity both at medium to short wavelength and at long wavelength, which well describes the strong purple-to-red nature of the colorant. The broader reflectance curves for Aronia L well represent its less specific coloration, being reddish brown in nature.

## 4. Discussion

ANCs, when extracted, exhibit lower stability compared to when held within the intact berry structure. Once

isolated, ANCs are prone to degradation or change influenced by environmental factors like pH and ionic content in suspension, and temperature and light exposure, ultimately diminishing both their health-promoting attributes and colorant applications.

Aronia L particles were larger than those of Aronia F, and for both types of Aronia an increase of diameter is seen with addition of $Ca^{2+}$ ions due to the possibility of coagulation between ANCs and pectin and $Ca^{2+}$ ion at lower pH (Borowska, et al., 2020; Fu, et al., 2023). The presence of $Ca^{2+}$ ions has been observed to exert a significant impact on the pH level of Aronia extract due to the neutralising effect of calcium salt production, consequently influencing the agglomeration dynamics within the suspension. This phenomenon plays a crucial role in moderating both the amount of flocculation and the size of agglomerated coagulates within the system. In general, increase in pH is likely to alter the surface charge of particles in the Aronia extract, leading to modifications in their colloidal behaviour due to the resulting effects on the electrostatic and van der Waals forces governing particle interactions, thereby influencing the agglomeration state of the suspension.

A comparative analysis of the reflectance changes between tablets fabricated from calcium carbonate ($CaCO_3$) and those composed of rutile titanium dioxide ($TiO_2$) reveals intriguing insights. The variations in reflectance can be indicative of differences in the optical properties, surface characteristics, or composition of the two types of tablets. On the one hand, the tablets made from $CaCO_3$ may exhibit distinct reflectance patterns, potentially associated with the birefringent interaction of light with the crystalline structure of calcite, a property not studied within the scope of this current work. On the other hand, tablets consisting of $TiO_2$ might display different interactive dye reflectance profiles across the pH related changes in dye coloration due to the unique photon exchange optical properties of titanium dioxide (Błaszczyk, et al., 2021; Zhang, et al., 2023). The effect of pH could, therefore, indicate a difference in solar cell performance if used in such photosensitising applications, in respect to shift in colour spectrum from purple to red, for low pH of 4.7, towards blue, at 7.4, and yellow at 10.4 (Woo, et al., 2021). Similarly, current density would likely be affected, depending on amount of molecular constitution changes (Fan, et al., 2019; Khan, et al., 2015; Wathon, et al., 2019). Further study understanding these reflectance changes would provide valuable information for applications such as pharmaceutical tablet identification and product encoding, quality control, and the assessment of material characteristics (Fu, et al., 2023; Liu, Fang and Ng, 2023).

Considering the diffuse reflectivity behaviour resulting from dye–substrate structure interaction in combination with the spectral changes undergoing by the dye as a function of pH and $Ca^{2+}$ exposure, it is clear that printing acidic natural plant dye inks onto modern alkaline substrates is challenging, not only in respect to long time colour fastness, but also in respect to colour gamut and photocatalytic effects.

### 4.1 Proposal of how to cope with the challenges

Resulting from the work presented in this paper, we undertake to make a short series of process proposals, which could be useful to the industry when attempting to fulfil the growing demand for the use of printing inks derived from natural plant dyes, especially when considering inkjet printing.

(i) Control pH of the ink in advance by a dilute base, simultaneously carefully analysing the spectral properties of the ink at pH ~ 8.8 as defining the end point coloration.

(ii) Promote rapid ink drying on $CaCO_3$ containing papers to prevent excessive saponification and ink particle coagulation. To achieve this, adopt highly porous coatings with strong capillarity, i.e. promote the presence of ultrafine pores.

(iii) Preferably use small volumes of ink, spatially densely applied. This latter requires increased jetting frequency to provide full tone areas through printed dot merging prior to rapid drying.

(iv) Adopt a strategy to buffer the $CaCO_3$, rendering it acid tolerant by capturing $Ca^{2+}$ released during acid interaction, thus maintaining the surrounding ambient acid pH of the ink. This is known to be achievable by combining the chelating action of reactive species, such as polyacrylate and/or polyamide groups with a weak base, such as considered in (i) above. The effect will be enhanced naturally by the weak to medium strong acidic properties of the dye itself, following the principle described by Wu (1997). Such a chelating agent in combination with the conjugate base could be used as part of the acid ink formulation. Testing this approach is, therefore, a subject for further work.

The main advantages of investing in natural ink dye products for functional printing of, for example, electronics and photosensitive energy production and storage devices are the low cost of the technology, the potential to recover device components and recycle the substrate as well as the active materials, following circular economy precepts, and rendering the product environmentally harmless whilst promoting biocompatible and naturally degradable devices (Okello, et al., 2022). Open Sound Control (OSC) as protocol for data transport specification and encoding during real-time

message communication among applications and hardware or electronic paper are already becoming commercially demanded products. Prototypes of devices like paper batteries, solar cells, nanopaper transistors, thermoelectric nanogenerators, graphene-enabled optoelectronics, biosensors, and even microfluidic lab-on-chip devices are under ongoing development. In these applications, paper can be used simply as the flexible substrate onto which researchers transfer thin-films, nanoparticles, or other nanostructures via various processes such as printing.

The value of considering pH sensitive dyes as sensors for a range of applications has already been recognised, especially, as mentioned earlier, when considering storage stability of perishable materials (Singh, Gaikwad and Lee, 2018). However, inverting the argument of coloration sensitivity from sensor to image reproduction results in a fascinating opportunity. As shown here, ANC dye can adopt a wide range of colours depending on its chemical and physical surrounding matrix (porous substrate) properties. The range closely approximates the standard cyan–magenta–yellow (CMY) component criteria for CMYK four colour printing. Deficiency in precise colour summation might be correctable by addition of further dyestuff to achieve full colour gamut.

Alternatively, if a method could be found to fix the dye to a substrate component(s), or component in solution, in such a way that the sensitivity of coloration to further chemical environmental change is suppressed, the hypothesis of covering the colour gamut with a single green-chemistry source could lead to a fully sustainable, biodegradable printing ink set structure.

A further alternative to chemically fixing the dye, and even more novel, could be to print a single pH sensitive dye at all pixel dots of an image. Then, virtually simultaneously, in alignment print the suitable activating pH-defined buffer as a secondary ink to generate in-situ the necessary coloured pixel. Each buffer could be selected from the complementing pH range needed to be applied to generate the respective dye response colours. In this way, the complete desired coloured image could be generated.

## 5. Conclusions

It is especially in the field of functional printing on modern available substrates where the challenges arise applying acidic plant dye ink onto porous alkaline filled or coated substrate. Understanding the interactions at play can enable the practitioner to predict and counter undesirable effects affecting process choice and runnability, economics, end product quality and its place in circular economy with focus on minimising or eliminating environmental impact. Following procedures such as those demonstrated in this current study can provide a framework for building the necessary control mechanisms to ensure application success. The result being, as hereby illustrated, that a simple action flowchart of checks and analyses can be generated for specific cases, and necessarily implemented under a policy of continuous process improvement to meet the emerging challenges within the functional print industry. Opportunities for applying natural plant dye inks are continuing to grow, and exploration of their interactions with environmental factors effecting and affecting the functionality of printed devices will remain a fertile area for further development. We can thus conclude that, in accordance with the title of this paper – 'natural plant dye inks set new challenges' – the opportunity to extend the boundaries of these challenges remains an exciting prospect for novel technology, not only supporting already identified applications but even considering full colour imaging from a single, or complementary, plant dye by post adjustment of pH and fixation. Such opportunities also extend to other photo-functionalities.

### References

Angelova, V.R., Tabakov, S.G., Peltekov, A.B. and Ivanov, K.I., 2017. The effect of soil contamination on chemical composition and quality of aronia (Aronia melanocarpa). *International Journal of Agricultural and Biological Engineering*, 11(11), pp. 787–792.

Arya, P., Wu, Y., Wang, F., Wang, Z., Marques, G. C., Levkin, P. A., Nestler, B. and Aghassi-Hagmann, J., 2024. Wetting behavior of inkjet-printed electronic inks on patterned substrates. *Langmuir*, 40, pp. 5162–5173: https://doi.org/10.1021/acs.langmuir.3c03297.

Asbury, J. B., Anderson, N. A., Hao, E., Ai, X. and Lian T., 2003. Parameters affecting electron injection dynamics from ruthenium dyes to titanium dioxide nanocrystalline thin film. *The Journal of Physical Chemistry B*, 107(30), pp. 7376–7386. https://doi.org/10.1021/JP034148R.

Błaszczyk, A., Joachimiak-Lechman, K., Sady, S., Tański, T., Szindler, M. and Drygała, A., 2021. Environmental performance of dye-sensitized solar cells based on natural dyes. *Solar Energy*, 2(215), pp. 346–355. https://doi.org/10.1016/j.solener.2020.12.040.

Borowska, S., Tomczyk, M., Strawa, J. W. and Brzóska, M. M., 2020. Estimation of the chelating ability of an extract from Aronia melanocarpa L. Berries and its main polyphenolic ingredients towards ions of zinc and copper. *Molecules*, 25(7):1507. https://doi.org/10.3390/molecules25071507.

Cotabarren, I. M., Cruces, S. and Palla, C. A., 2019. Extrusion 3D printing of nutraceutical oral dosage forms formulated with monoglycerides oleogels and phytosterols mixtures. *Food Research International*, 126, pp. 108676–108687. https://doi.org/10.1016/j.foodres.2019.108676.

Dangles, O., Saito, N. and Brouillard, R., 1993. Anthocyanin intramolecular copigment effect. *Phytochemistry*, 34(1), pp. 119–124. https://doi.org/10.1016/S0031-9422(00)90792-1.

Dimić-Mišić, K., Karakoc, A., Ozkan, M., Hashmi, S. G., Maloney, T. and Paltakari, J., 2015. Flow characteristics of ink-jet inks used for functional printing. *Organic Electronics*, 38, pp. 307–315. https://doi.org/10.1016/j.orgel.2016.09.001.

Duffy, J. J., Hill, A. J. and Murphy, S. H., 2015. Simple method for determining stress and strain constants for non-standard measuring systems on a rotational rheometer. *Applied Rheology*, 25(4), pp. 8–13. https://doi.org/10.3933/applrheol-25-42670.

Fan, H., Zhang, M., Liu, Z. and Ye, Y., 2019. Effect of microwave-salt synergetic pre-treatment on the 3D printing performance of SPI-strawberry ink system. *LWT*, 122:109004. https://doi.org/10.1016/j.lwt.2019.109004.

Fu, W., Li, S., Helmick, H., Hamaker, B. R., Kokini, J. L. and Reddivari, L., 2023. Complexation with polysaccharides enhances the stability of isolated ANCs. *Foods*, 12(9):1846. https://doi.org/10.3390/foods12091846.

Gane, P.A.C. and Koivunen, K., 2010. Relating liquid location as a function of contact time within a porous coating structure to optical reflectance. *Transport in Porous Media*, 84, pp. 587–603. https://doi.org/10.1007/s11242-009-9523-x.

Gane, P.A., Imani, M., Dimić-Mišić, K., and Kerner, E., 2021. Novel device for determining the effect of jetting shear on the stability of inkjet ink. *Journal of Print and Media Technology Research*, 10(1), 7–24. https://doi.org/10.14622/JPMTR-2015.

Hakim, L., Deshmukh, R.K., Lee, Y.S. and Gaikwad, K.K., 2024. Edible ink for food printing and packaging applications: a review. *Sustainable Food Technology*, 2, pp. 876–892. https://doi.org/10.1039/d4fb00036f.

Hashmi, S.G., Ozkan, M., Halme, J., Dimic Misic, K., Zakeeruddin, S.M., Paltakari, J., Grätzel, M. and Lund, P.D., 2015. High performance dye-sensitized solar cells with inkjet printed ionic liquid electrolyte. *Nano Energy*, 17, pp. 206–215. https://doi.org/10.1016/j.nanoen.2015.08.019.

Hellström, J.K., Shikov, A.N., Makarova, M.N., Pihlanto, A.M., Pozharitskaya, O.N., Ryhänen, E–L., Kivijärvi, P., Makarov, V.G. and Mattila, P.H., 2010. Blood pressure-lowering properties of chokeberry (Aronia mitchurinii, var. Viking). *Journal of Functional Foods*, 2(2), pp. 163–169. https://doi.org/10.1016/j.jff.2010.04.004.

Henneberg, M. and Stasrznewicz, M., 1993. Herbal ethnopharmacology of Lithuania/Vilnius region III: Medicament and Food. In: *Actes du 2e Colloque Européen d'Ethnopharmacologie et de la Conférence Internationale d'Ethnomédecine*, Heidelberg, 1993. Paris: IRD Éditions, pp. 243–255.

Huang, S., Basore, P., Boyd, M., Jones-Albertus, B., Nilsen, G., Silverman, T., Sodano, D. and Tinker, L., 2022. *Solar Energy Technologies Office Photovoltaics End-of-Life Action Plan*. US Department of Energy, Office of Energy Efficiency and Renewable Energy, DOE/EE-2571: energy.gov/eere/solar.

Huang, R. and Xu, C. (2023). Sensory property and phenolic profile of aronia juice. In: Mérillon, JM., Riviere, C., Lefèvre, G. (eds) *Natural Products in Beverages*. Reference Series in Phytochemistry. Springer, Cham. https://doi.org/10.1007/978-3-031-04195-2_73-1.

Hwang, B. H., Sakakibara, A. and Miki, K., 1981. Hydrogenolysis of Protolignin-XVII. Isolation of three dimeric compounds with y–0–4, ß–1, and ß–0–4 linkages from hardwood lignin. *Holzforschung*, 35(5), pp. 229–232. https://doi.org/10.1515/hfsg.1981.35.5.229.

Imanishi, A., Okamura, T., Ohashi, N., Nakamura, R. and Nakato, Y., 2007. Mechanism of water photooxidation reaction at atomically flat $TiO_2$ (rutile) (110) and (100) surfaces: dependence on solution pH. *Journal of the American Chemical Society*, 129(37), pp. 11569–11578. https://doi.org/10.1021/ja073206.

Jurič, I., Karlović, I., Tomić, I. and Novaković, D., 2013. Optical paper properties and their influence on colour reproduction and perceived print quality. *Nordic Pulp & Paper Research Journal*, 28(2), pp. 264–273. https://doi.org/10.3183/npprj-2013-28-02-p264-273.

Kampuse, S., Krūma, Z., Kampuss, K. and Krasnova, I., 2009. Nutritional value of minor fruits in Latvia. *Acta Horticulturae*, 877: pp. 1221–1228. https://doi.org/10.17660/ActaHortic.2010.877.166.

Khan, M.Z., Al–Mamun, M.R., Al-Amin, M., Moniruzzaman, M. and Hasan, M.R., 2015. Dye-sensitized solar cell using used semiconductor glass and natural dye: towards alternative energy challenge. *International Journal of Renewable Energy*, 5(2), pp. 38–44.

Khoo, H.E., Azlan, A., Tang, S.T. and Lim, S.M., 2017. Anthocyanidins and ANCs: Colored pigments as food, pharmaceutical ingredients, and the potential health benefits. *Food & Nutrition Research*, 61(1):1361779. https://doi.org/10.1080/16546628.2017.1361779.

Koivunen, K. and Gane, P.A.C., 2010. Optical reflectance as a function of liquid contact time and penetration depth distribution in coatings with mono and discretely bimodal pore size distributions, *Proceedings of the 2010 TAPPI Advanced Coating Fundamentals Symposium*, TAPPI Press, Atlanta GA, pp. 108–128.

Koivunen, R., Jutila, E. and Gane, P., 2015. Inkjet printed hydrophobic microfluidic channelling on porous substrates. *Journal of Print and Media Technology Research*, 4(1), pp. 7–17. https://doi.org/10.14622/JPMTR-1413.

Leonard, P.J., Brand, M.H., Connolly, B.A. and Obae, S.G., 2013. Investigation of the origin of Aronia mitschurinii using amplified fragment length polymorphism analysis. *Hort. Science*, 48(5), pp. 520–524. https://doi.org/10.21273/HORTSCI.48.5.520.

Liu, S., Fang, Z. and Ng, K., 2023. Recent development in fabrication and evaluation of phenolic-dietary fiber composites for potential treatment of colonic diseases. *Critical Reviews in Food Science and Nutrition*, 63(24), pp. 6860–6884. https://doi.org/10.1080/10408398.2022.2043236.

Mahmood, K., Alamri, M. S., Abdellatif, M. A., Hussain, S., Qasem, A. A., 2018. Wheat flour and gum cordia composite system: Pasting, rheology and texture studies. *Food Science Technology*, 38, pp. 691–697. https://doi.org/10.1590/FST.10717.

Mary, S.K., Koshy, R.R., Daniel, J., Koshy, J.T., Pothen, L.A. and Thomas, S., 2020. Development of starch based intelligent films by incorporating ANCs of butterfly pea flower and $TiO_2$ and their applicability as freshness sensors for prawns during storage. *RSC Advances*, 10(65), pp. 39822–39830. https://doi.org/10.1039/d0ra05986b.

McKay, S.A., 2001. Demand increasing for Aronia and elderberry in North America. *New York Fruit Quarterly*, 9(3), pp. 2–3.

Medina-Meza, I.G., Boioli, P. and Barbosa-Cánovas, G. V., 2016. Assessment of the effects of ultrasonics and pulsed electric fields on nutritional and rheological properties of raspberry and blueberry purees. *Food and Bioprocess Technology*, 9, pp. 520–531. https://doi.org/10.1007/s11947-015-1642-5.

Miki, J., Asanuma, M., Tachibana, Y. and Shikada, T., 1995. Novel catalyst systems for phenol synthesis by vapor phase oxidation of benzoic acid. *Bulletin of the Chemical Society of Japan*, 68(8), pp. 2429–2437. https://doi.org/10.1006/jcat.1995.1034.

Mossberg, B., Stenberg, L., Vuokko, S. and Väre, H. (eds), 2005, *Suuri Pohjolan kasvio*. Tammi, Helsinki.

Okello, A., Owuor, B. O., Namukobe, J., Okello, D. and Mwabora, J., 2022. Influence of the pH of ANCs on the efficiency of dye sensitized solar cells. *Heliyon*, 8(7):e09921. https://doi.org/10.1016/j.heliyon.2022.e09921.

Özkan, M., Dimic-Misic, K., Karakoc, A., Hashmi, S.G., Lund, P., Maloney, T. and Paltakari, J. 2016. Rheological characterization of liquid electrolytes for drop-on-demand inkjet printing. *Organic Electronics.* 38, pp. 307–315. https://doi.org/10.1016/j.orgel.2016.09.001.

Perišić, M., Barceló, E., Dimić-Mišić, K., Imani, M. and Spasojević Brkić, V., 2022. The role of bioeconomy in the future energy scenario: a state-of-the-art review. *Sustainability*, 14(1):560. https://doi.org/10.3390/su14010560.

Ridgway, C.J. and Gane, P.A.C., 2005. Ink-coating adhesion: the importance of pore size and pigment surface chemistry. J*ournal of Dispersion Science and Technology*, 25(4), pp. 469–480. https://doi.org/10.1081/DIS-200025717.

Ridgway, C. J., Schoelkopf, J. and Gane, P. A. C., 2003. A new method for measuring the liquid permeability of coated and uncoated papers and boards. *Nordic Pulp & Paper Research Journal*, 18(4), pp. 377–381. https://doi.org/10.3183/npprj-2003-18-04-p377-381.

Rousseau, J., 1945. Le folklore botanique de Caughnawaga. *Contributions de l'Institut botanique l'Universite de Montreal*, 55, pp. 7–72.

Rousseau, J., 1947. Ethnobotanique abenakise. *Archives de Folklore*, 11, pp. 145–182.

Sant'Anna, V., Gurak, P.D., Marczak, L.D. and Tessaro, I.C., 2013. Tracking bioactive compounds with colour changes in foods-A review. *Dyes and Pigments*, 98(3), pp. 601–608. https://doi.org/10.1016/j.dyepig.2013.04.011.

Sarv, V., Venskutonis, P. R., Rätsep, R., Aluvee, A., Kazernavičiūtė, R. and Bhat, R., 2021. Antioxidants characterization of the fruit, juice, and pomace of sweet rowanberry (Sorbus aucuparia l.) cultivated in Estonia. *Antioxidants*, 10(11):1779. https://doi.org/10.3390/antiox10111779.

Schön, C., Mödinger, Y., Krüger, F., Doebis, C., Pischel, I. and Bonnländer, B., 2021. A new high-quality elderberry plant extract exerts antiviral and immunomodulatory effects in vitro and ex vivo. *Food and Agricultural Immunology*, 32(1), pp. 650–662. https://doi.org/10.1080/09540105.2021.1978941.

Singh, S., Gaikwad, K. K., and Lee, Y. S., 2018. Anthocyanin – A natural dye for smart food packaging systems. *Korean Journal of Packaging Science and Technology*, 24(3), pp. 167–180. https://doi.org/10.20909/kopast.2018.24.3.167.

Skupien, K., Ochmian, I. and Grajkowski, J., 2008. Influence of mineral fertilization on selected physical features and chemical composition of aronia fruit. *Acta Agrophysica*, 11(1), pp. 213–226.

Smith, H.H., 1933*.* Ethnobotany of the forest potawatomi indians*. Bulletin of the Public Museum of the City of Milwaukee,* 7, pp. 1–230.

Sokolov, S.Y. (2000) Phytotherapy and phytopharmacology: a guide for doctors. *Medical news Agency*, Moscow, 976.

Taheri, R., Connolly, B. A., Brand, M. H. and Bolling, B. W., 2013. Underutilized chokeberry (Aronia melanocarpa, Aronia arbutifolia, Aronia prunifolia) accessions are rich sources of ANCs, flavonoids, hydroxycinnamic acids, and proanthocyanidins. *Journal of Agricultural and Food Chemistry*, 61(36), pp. 8581–8588. https://doi.org/10.1021/jf402449q.

Tahir, H. and Saad, M., 2021. Chapter 3 – Using dyes to evaluate the photocatalytic activity. In: M. Ghaedi, ed. *Interface Science and Technology*. 32nd ed. [online], pp. 125–224. https://doi.org/10.1016/B978-0-12-818806-4.00005-X.

Tolić, M-T., Jurčević, I., L., Krbavčić I. P., Marković, K. and Vahčić, N., 2015. Phenolic content, antioxidant capacity and quality of chokeberry (Aronia melanocarpa) products. *Food Technology and Biotechnology*, 53(2), pp. 171–179. https://doi.org/10.17113/ftb.53.02.15.3833.

Vandeput, B., 2021. *Baroa belaobara: berryapple*. PhD. Aalto University. Department of Art. *University Publication Series Doctoral Dissertations*, 65/2021. Available at: https://aaltodoc.aalto.fi/items/d210ecd3-031c-4c15-bc42-6960c21abcfb [Accessed 10 December 2024].

Vatai, T., Škerget, M., Knez, Ž., Kareth, S., Wehowski, M. and Weidner, E., 2008. Extraction and formulation of anthocyanin-concentrates from grape residues. *The Journal of Supercritical Fluids*, 45(1), pp. 32–36. https://doi.org/10.1016/j.supflu.2007.12.008.

Velmurugan, P., Vedhanayakisri, K. A., Park, Y. J., Jin, J. S. and Oh, B. T., 2019. Use of Aronia melanocarpa fruit dye combined with silver nanoparticles to dye fabrics and leather and assessment of its antibacterial potential against skin bacteria. *Fibers Polymers,* 20, pp. 302–311. https://doi.org/10.1007/s12221-019-8875-2.

Wathon, M.H., Beaumont, N., Benohoud, M., Blackburn, R.S. and Rayner, C.M., 2019. Extraction of ANCs from Aronia melanocarpa skin waste as a sustainable source of natural colorants. *Color Technology*, 135(1), pp. 5–16. https://doi.org/10.1111/cote.12385.

Woo, H.W. and Lee, J.S, 2021. Characterization of electrospun Aronia melanocarpa fruit extracts loaded polyurethane nanoweb. *Fashion and Textiles*, 8, pp. 1–4. https://doi.org/10.1186/s40691-021-00250-z.

Wu, K.T., 1997. *Acid resistant calcium carbonate filler*; ECC International Inc., WO 97/08247.

Zhang, P., Chu, F., Zhou, M., Tao, B. and Miao, F., 2024. DSSC using natural dye sensitized and Ag/CdS/$TiO_2$ composite structured light anode. *Vacuum*, 219:112763. https://doi.org/10.1016/j.vacuum.2023.112763.

Živković, I.P., Jurić, S., Vinceković, M., Galešić, M.A., Marijan, M., Vlahoviček-Kahlina, K., Mikac, K. M. and Lemic, D. 2020. Polyphenol-based microencapsulated extracts as novel green insecticides for sustainable management of polyphagous brown marmorated stink bug (Halyomorpha halys Stål, 1855). *Sustainability*, 12(23):10079. https://doi.org/10.3390/su122310079.